

densities, very well represented by eq 18, are recovered.

Conclusions

All chains examined, and in our conviction all flexible linear chains, are characterized by bimodal three-dimensional segment density distributions at high segment densities. For all chains the measures of shape indicate a high shape anisotropy for short chain length that decreases within a few hundred skeletal bonds to the limiting values. Long chains at low segment densities resemble a cake of soap, while the detailed shape of short- and medium-length polymers is very dependent on structural details.

Acknowledgment. This work was supported by NSF Grant DMR-8312694 and the Texaco-Manglesdorf Associate Professorship in the Department of Chemical Engineering at MIT. We thank Professors Mattice and Šolc for helpful discussions.

Appendix. Radius of Gyration Tensor and the Reduced Moment of Inertia Tensor

The moment of inertia tensor of a chain, consisting of $n + 1$ "atoms" of equal mass, reduced by the total mass of the chain, is¹⁸

$$\mathbf{I} = \frac{1}{n+1} \sum_{i=0}^n \begin{bmatrix} y^2 + z^2 & -xy & -xz \\ -xy & z^2 + x^2 & -yz \\ -xz & -yz & x^2 + y^2 \end{bmatrix} = \text{tr}(\mathbf{S})\mathbf{E} - \mathbf{S}$$

where \mathbf{E} is the unit tensor. Hence both \mathbf{I} and \mathbf{S} are diagonal in the same principal axis system, and in this frame of reference

$$\mathbf{I} = \text{diag}(\bar{Y}^2 + \bar{Z}^2, \bar{Z}^2 + \bar{X}^2, \bar{X}^2 + \bar{Y}^2)$$

where \bar{X}^2 , \bar{Y}^2 , and \bar{Z}^2 are the eigenvalues of \mathbf{S} , and $\text{tr}(\mathbf{I})$

$$= 2 \text{ tr}(\mathbf{S}).$$

References and Notes

- (1) Debye, P.; Bueche, F. *J. Chem. Phys.* **1952**, *20*, 1337-8.
- (2) Flory, P. J. "Principles of Polymer Chemistry"; Cornell University Press: Ithaca, NY, 1953; Chapter XII.2.
- (3) Flory, P. J. "Statistical Mechanics of Chain Molecules"; Interscience: New York, 1969; Chapter VIII.
- (4) Yamakawa, H. "Modern Theory of Polymer Solutions"; Harper and Row: New York, 1971; Chapter II.7.
- (5) Kuhn, W. *Kolloid-Z.* **1934**, *68*, 2-15.
- (6) Yoon, D. Y.; Flory, P. J. *J. Chem. Phys.* **1974**, *61*, 5366-80.
- (7) Šolc, K. *Polym. News* **1977**, *4*, 67-74.
- (8) Šolc, K.; Stockmayer, W. H. *J. Chem. Phys.* **1971**, *54*, 2756-7.
- (9) Šolc, K. *J. Chem. Phys.* **1971**, *55*, 335-44.
- (10) Koyama, R. *J. Phys. Soc. Jpn.* **1968**, *24*, 580-8.
- (11) Mattice, W. *J. Am. Chem. Soc.* **1979**, *101*, 732-6.
- (12) Mattice, W. *J. Am. Chem. Soc.* **1979**, *101*, 7651-4.
- (13) Mattice, W. *Macromolecules* **1979**, *12*, 944-8.
- (14) Mattice, W. *Macromolecules* **1980**, *13*, 904-9.
- (15) Mattice, W. *Macromolecules* **1981**, *14*, 863-7.
- (16) Rubin, R. J.; Mazur, J. *Macromolecules* **1977**, *10*, 139-49.
- (17) The j th invariant of a tensor \mathbf{A} , with eigenvalues λ_1 , λ_2 , and λ_3 , is defined as the sum of all subdeterminants of order j , i.e.

$$I_1 = \lambda_1 + \lambda_2 + \lambda_3 = \text{tr}(\mathbf{A})$$

$$I_2 = \lambda_1\lambda_2 + \lambda_2\lambda_3 + \lambda_3\lambda_1$$

$$I_3 = \lambda_1\lambda_2\lambda_3 = \det(\mathbf{A})$$
- (18) Landau, L. D.; Lifshitz, E. M. "Course of Theoretical Physics", 3rd ed.; Pergamon Press: Elmstord, NY, 1976; Volume 1, Chapter VI.
- (19) Smith, R. P.; Mortensen, E. M. *J. Chem. Phys.* **1960**, *32*, 502-7.
- (20) Flory, P. J. *Macromolecules* **1974**, *7*, 381-92.
- (21) Suter, U. W.; Flory, P. J. *Macromolecules* **1975**, *8*, 765-76.
- (22) Chapter III.8 of ref 3.
- (23) Flory, P. J.; Abe, Y. *J. Chem. Phys.* **1971**, *54*, 1351-63. Also: Nagai, K. *J. Chem. Phys.* **1968**, *48*, 5646-55.
- (24) Wright, T. J. *Comput. Graphics* **1979**, *13*, 182-9; subroutine ISOSRF of the SCD Graphics System of the National Center for Atmospheric Research, Boulder, Co.
- (25) Reference 4, p 26. Also: Gobush, W.; Šolc, K.; Stockmayer, W. H. *J. Chem. Phys.* **1974**, *60*, 12-21.
- (26) Zimm, B. H. *Macromolecules* **1980**, *13*, 592-602.

Uniaxial Draw of Poly(ethylene oxide) by Solid-State Extrusion

Bong Shik Kim and Roger S. Porter*

Polymer Science and Engineering Department, Materials Research Laboratory, University of Massachusetts, Amherst, Massachusetts 01003. Received October 1, 1984

ABSTRACT: Ultradrawn filaments of poly(ethylene oxide) (PEO) have been prepared by a solid-state coextrusion in an Instron capillary rheometer. Two different molecular weights, 3.0×10^5 and 4.0×10^6 , were evaluated. Properties have been examined as a function of uniaxial draw ratio. The drawn filaments of PEO exhibit extremes of melting point, percent crystallinity, birefringence, and tensile modulus. Features of a PEO filament with a draw ratio of 32 are a 72 °C DSC melting point and a crystallinity of 94.0%, both measured at a scan of 2.5 °C min⁻¹. The corresponding birefringence is 3.5×10^{-2} and the Young's modulus 3.5 GPa.

Introduction

Extrusion of several thermoplastics in the crystalline state has been performed over this past decade.^{1,2} A purpose of these studies has been to produce highly oriented morphologies. Despite the great interest in polymer drawing, few studies on poly(ethylene oxide) (PEO) have been reported. Kitao et al.^{3,4} employed two different drawing methods: (1) a dry and a wet process each at different temperatures; (2) a melt spinning method. A relatively low draw ratio (7.9), percent crystallinity, and birefringence were reported.

To obtain higher draw ratios and to achieve enhance physical properties, strands of PEO were drawn in this

study by solid-state coextrusion by a technique reported by Griswold et al.⁵ PEO extrudates of high draw resulting in filaments have been evaluated by thermal analysis, mechanical properties, and birefringence. The method of draw has the advantage of extensional deformation, under pressure and on a substrate for stress distribution.⁵⁻⁷

Experimental Section

The samples of PEO used in this study were obtained in powder form from Polyscience, Inc., Pittsburgh, PA. The molecular weights, \bar{M}_w , of the poly(ethylene oxide) samples were reported to be 3.0×10^5 and 4.0×10^6 . The powders were compression molded for 20 min at 110 °C and 15 000 psi into sheets of 0.2-0.3-mm thickness followed by cooling to ambient. At this stage

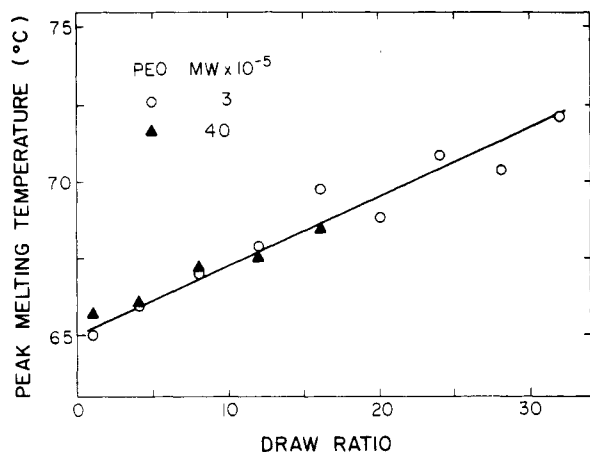


Figure 1. Effect of draw ratio on the peak melting temperature at a heating rate of $2.5\text{ }^{\circ}\text{C min}^{-1}$. PEO drawn at $40\text{ }^{\circ}\text{C}$: (○) $\bar{M}_v = 3.0 \times 10^5$; (▲) $\bar{M}_v = 4.0 \times 10^6$.

atmospheric moisture was not considered a problem. Samples were extrusion drawn by using solid-state coextrusion as described earlier.⁵⁻⁷ Briefly, in this process a ribbon cut from the poly(ethylene oxide) sheet is inserted into $3/8$ in. diameter polyethylene billets which had been split longitudinally. This assembly was then press fitted into the barrel of an Instron capillary rheometer and then pushed through conical brass dies of 20° included entrance angle. The ratio of the cross-sectional area at the top of the cone to that at the bottom of the cone provides a draw ratio up to 8. This value agrees with that calculated from the displacement of transverse marks made on the PEO ribbon as a consequence of draw; the ratio reported here may be up to 10% lower because of differential draw between the PEO ribbon and the polyethylene billet. The higher draw ratios were obtained by drawing again the same PEO ribbons within fresh polyethylene billets. Extrusion was evaluated at several temperatures from ambient to the PEO melting point. Extrusion drawing was found to be most effectively carried out at $40\text{ }^{\circ}\text{C}$, well below the PEO melting point. This temperature led to the highest draw ratio for PEO. The extrusion rate was $\sim 0.01\text{ cm min}^{-1}$. Solid-state extrusions at $50\text{ }^{\circ}\text{C}$ were less successful possibly because of relaxation processes.

The thermal analysis instrument used was a computerized (TADS) Perkin-Elmer DSC-2. The DSC was calibrated by using ice and pure indium. Birefringence measurements were made at room temperature by using a Zeiss polarizing microscope equipped with a Zeiss calcspars tilting compensator and a white light source ($5500\text{-}\text{\AA}$ wavelength). Tensile tests were made at ambient on the drawn PEO ribbons by using an Instron testing machine, Model TTM, at a cross-head speed of 0.1 cm min^{-1} . The initial sample length was 50 mm. Tensile modulus was calculated as the tangent to the stress-strain curve at a strain of 0.1%.

Results and Discussion

The highly drawn PEO ribbons exhibited a range of interesting properties. The most striking result of the DSC studies is the observance of uniquely high melting points. Figure 1 shows the effect of draw ratio on the endothermic peak melting temperature at a low scanning rate of $2.5\text{ }^{\circ}\text{C min}^{-1}$. The melting point increases with uniaxial draw from $65\text{ }^{\circ}\text{C}$ reaching $72\text{ }^{\circ}\text{C}$ at a draw ratio of 32. The melting point appears to have not yet reached a limit with draw and is significantly higher than those previously published for PEO. Lang et al.⁸ have reported that an unannealed PEO melts at $65\text{ }^{\circ}\text{C}$. Mandelkern et al.⁹ have given a value of $66\text{ }^{\circ}\text{C}$ and Porter and Boyd¹⁰ a value of $62\text{ }^{\circ}\text{C}$. Beech and Booth¹¹ reported a melting temperature of $69.2\text{ }^{\circ}\text{C}$ for a well-annealed, high molecular weight fraction of PEO.

Nedkov et al.¹² have carried out DSC experiments on nascent PEO. They reported melting points for the newly formed PEO ranging from $\sim 66\text{ }^{\circ}\text{C}$ for a molecular weight

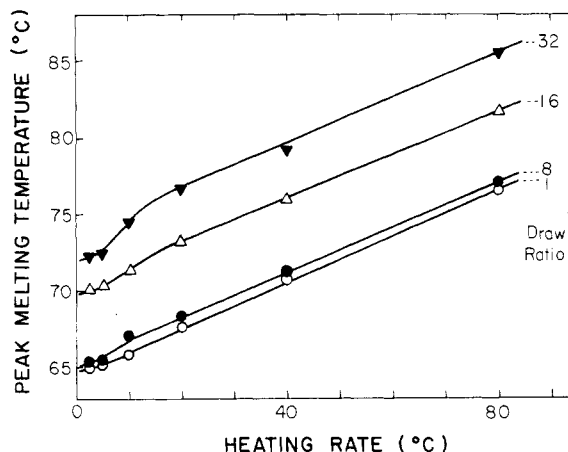


Figure 2. Effect of heating rate on the peak melting temperature of undrawn film and drawn films of PEO $\bar{M}_v = 3.0 \times 10^5$.

of 1.75×10^6 to $70\text{ }^{\circ}\text{C}$ for a molecular weight of 7.0×10^6 . Over this molecular weight range, they found a linear relationship between molecular weight and melting temperature. However, upon second heating the melting points for their samples were found to range from slightly less than $66\text{ }^{\circ}\text{C}$ for molecular weight of 1.75×10^6 to $63\text{ }^{\circ}\text{C}$ for molecular weight of 7.0×10^6 . The high melting points for the nascent samples were ascribed to the influence of tie molecules which were thought, because of polymerization conditions, to be linking lamellae. After the initial melting it is postulated that these tie molecules were reduced.

The melting points reported here may also be compared to those predicted for an infinitely-extended-chain crystal of PEO. Buckley and Kovacs¹³ calculate a theoretical melting point of $64 \pm 0.4\text{ }^{\circ}\text{C}$. Beech and Booth¹¹ offer a value of $76\text{ }^{\circ}\text{C}$. This layer value was obtained by extrapolation of their data for melting point and crystallization temperature. Lang et al.⁸ report $74\text{ }^{\circ}\text{C}$, derived from an extrapolation of peak melting temperature changes with annealing temperature. The maximum melting point of $72.1\text{ }^{\circ}\text{C}$ obtained here, at a draw ratio of 32, thus approaches values derived for a fully chain extended crystal. The increase of melting point with draw ratio is consistent with an entropy constraint in the noncrystalline regions that increases with drawing or alternatively viewed simply as increased crystal perfection.

The effect of heating rate on peak melting temperature for the PEO of molecular weight 3.0×10^5 is shown in Figure 2. The melting temperatures observed at heating rates $< 5\text{ }^{\circ}\text{C min}^{-1}$ are essentially unaffected, but melting temperatures measured at higher rates increase monotonically with heating rates. Since the slopes reported in Figure 2 are independent of draw ratio, superheating effects are likely small. Thus, the observed heating rate effect is likely due mainly to heat transfer rather than to the PEO morphology. The curvature in the plots at low draw is likely the result of annealing during slow heating. According to Clements et al.¹⁴ and Jaffe et al.,¹⁵ in oriented polymers superheating effects are attributable to the entropic restriction on molecular chains that connect two or more crystalline regions of the same or different crystals.

The monotonic increase in crystallinity in PEO on draw is shown in Figure 3. The percent crystallinity has been calculated from the heat of fusion as determined from the area under the fusion curve. The degree of crystallinity in percent is defined as¹⁶

$$\text{fraction crystallinity} = \Delta H_1 / \Delta H_2$$

where ΔH_1 is the heat of fusion of the partially crystalline

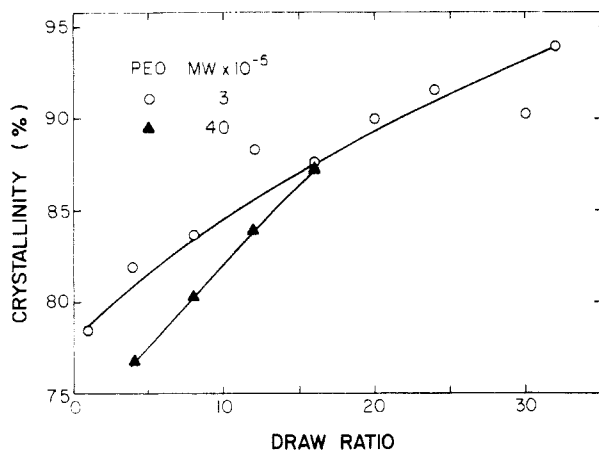


Figure 3. Effect of draw ratio on the percent crystallinity of PEO at a heating rate of 2.5 °C min⁻¹.

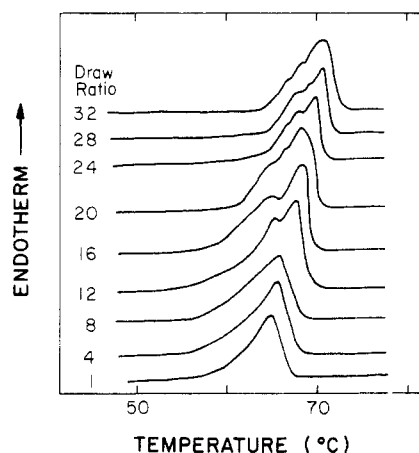


Figure 4. DSC endotherms at indicated draw ratio measured at a heating rate of 2.5 °C min⁻¹. $\bar{M}_v = 3 \times 10^5$.

specimen and ΔH_2 the heat of fusion of the perfect crystal. The percent crystallinity in this study has been computed by using 1980 cal/mol for ΔH_2 of PEO.^{9,17} The highest fractional crystallinity developed in this work is 94.0%, measured at a DSC scanning rate of 2.5 °C min⁻¹, and was 95.3% at a scanning rate 10 °C min⁻¹, both for a PEO draw ratio of 32. These values are higher than previously reported for drawn PEO, with a previous high cited of 85%.⁴

Multiple melting peaks are also a notable characteristic of the fusion curves for drawn PEO, as shown in Figure 4. Their appearance, however, is poorly reproducible. Irregularities in the melting endotherms first appear at a draw ratio of ~8 with yet more complex peaks noted at draw ratios ≥ 20 , but with the multiple peaks always disappearing on second heating of the previously drawn PEO.

Comparable features have been reported for drawn polyethylene,¹⁸⁻²⁰ except that superheating is also observed. Southern¹⁸ and Mead¹⁹ with co-workers associated dual melting peaks with the presence of both chain-folded and chain-extended crystals. Aharoni and Sibilis²⁰ associated the appearance of three melting peaks to the existence of three morphologies in the drawn extrudates.

Thermal crystallization²¹ and annealing⁸ of PEO are also known to produce multiple melting peaks. Buckley and Kovacs²¹ reported that this phenomenon can be assigned to the melting of once-folded and extended-chain crystals, with the higher endothermic peak corresponding to the extended chains. Lang et al.⁸ reported the lowest melting peak in PEO may be interpreted as a melting of a crystalline fraction formed by some "impurities", i.e., less regular components in fractions which tend to be rejected

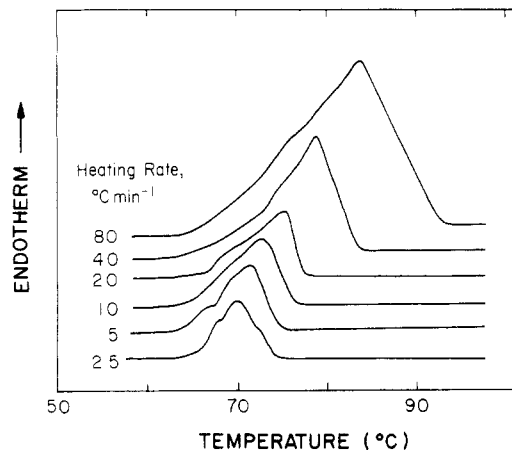


Figure 5. Endotherms for PEO ribbons of draw ratio 32 at indicated heating rates. $\bar{M}_v = 3.0 \times 10^5$.

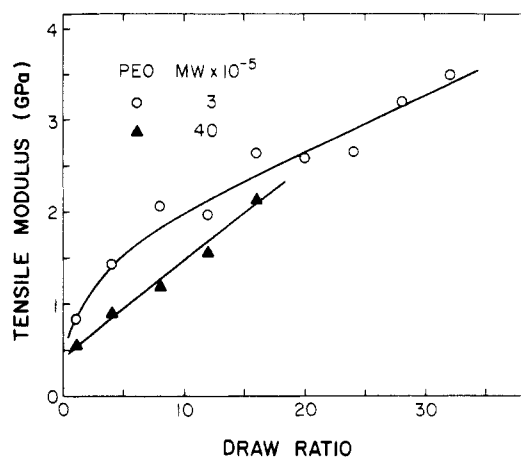


Figure 6. PEO tensile modulus as a function of draw ratio.

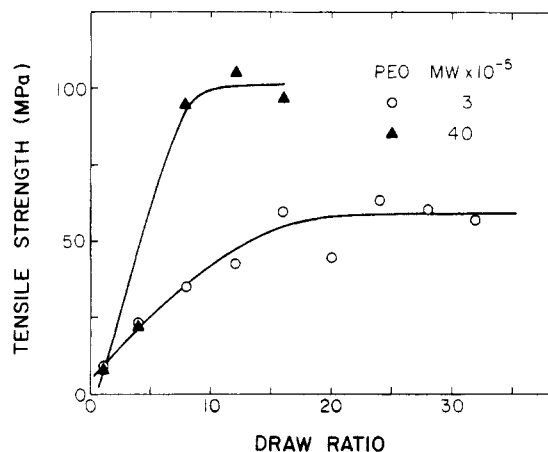


Figure 7. PEO tensile strength as a function of draw ratio.

during primary crystallization and thus crystallize separately during annealing. The next endotherm is attributed to the primary crystallization. The third peak has been ascribed to the melting of folded-chain crystals. The dual peaks observed here in ribbons drawn up to ratio of 32 are still evident even on analysis at a heating rate 80 °C min⁻¹, as shown in Figure 5.

Results of tensile modulus and strength, calculated from stress-strain curves, are shown in Figures 6 and 7. The tensile moduli and strengths are noted to increase with uniaxial draw. The highest tensile modulus attained is 3.5 GPa. This value far exceeds the highest previously reported value for drawn PEO fibers of 793 MPa.²² The

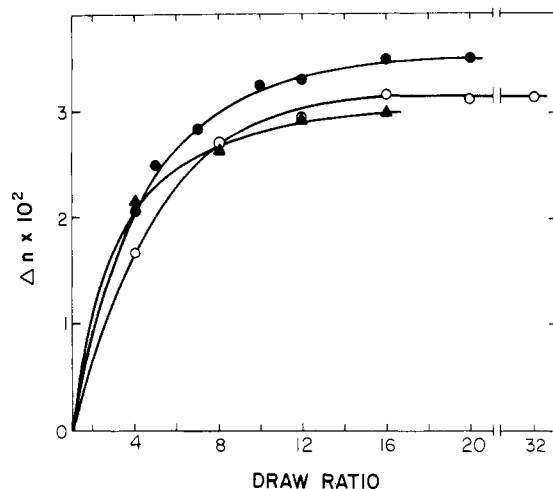


Figure 8. Birefringence of uniaxially drawn PEO film: (O) $\bar{M}_v = 3.0 \times 10^6$ and extrusion rate 0.01 cm min^{-1} , (●) $\bar{M}_v = 3.0 \times 10^6$ and extrusion rate 0.1 cm min^{-1} , (▲) $\bar{M}_v = 4.0 \times 10^6$ and extrusion rate 0.01 cm min^{-1} .

theoretical crystal modulus in the chain direction is inherently low because of the helical conformation of the chain.

The calculation of elastic moduli for PEO crystals in the chain direction has been reported to be 4.6–4.9 GPa.²³ In this calculation, a helical skeleton conformation model of PEO is used in which the internal rotation angles are taken to be all gauche. Sakurada²⁴ obtained an estimated maximum elastic modulus of 7.8–9.2 GPa for the crystal lattice of PEO in which the internal rotation angles were taken to be in trans–trans–gauche conformations.

The tensile moduli of the drawn PEO measured here and reported²⁵ are insensitive to choice of molecular weight. This is similar to the result of Perkins et al.²⁶ in which Young's modulus for drawn high-density polyethylene is essentially independent of molecular weight.

Figure 7 shows the change of PEO tensile strength with draw ratio. Here the tensile strength of high molecular weight PEO is much higher than that for the lower. This is also consistent with results on other polymers and in accordance with the proposal of Flory²⁷

$$\sigma = A - B/\bar{M}_n$$

where σ is tensile strength and the constants A and B vary with polymer composition and \bar{M}_n is the number-average molecular weight.

Birefringence has been chosen to evaluate the extent of orientation achieved on drawing by solid-state extrusion. The total birefringence $\Delta\eta_T$ of the extrudates was estimated from the equation²⁸

$$\Delta\eta_T = (R/d\lambda)$$

where d is the sample thickness, R is the retardation, and λ is the wavelength. As shown in Figure 8, birefringence increases steeply with draw at low values, but above a draw ratio of 16, $\Delta\eta_T$ approaches a plateau.²⁹ The highest value of birefringence attained here is 3.52×10^{-2} . This is higher than the highest prior report of 3.4×10^{-2} , for a drawn PEO

fiber.⁴ The birefringence measured on extrudates prepared at faster extrusion rates is higher than at low rates. This is likely related to more annealing at lower extrusion rates for the drawn ribbon on exiting the die at 40°C and without tension.³⁰ An even higher birefringence of 3.75 is reported in companion studies on independent samples.

Acknowledgment. This study was also supported in part by a grant to R.S.P. by the Office of Naval Research. B.S.K. acknowledges the financial support given by the Ministry of Education, Korea, during the period in which this research was undertaken.

References and Notes

- (1) N. J. Capiati, S. Kojima, W. G. Perkins, and R. S. Porter, *J. Mater. Sci.*, **12**, 334 (1977).
- (2) H. Ulrich, "Introduction to Industrial Polymers", Hanser, New York, 1981.
- (3) T. Kitao, K. Yamada, T. Yamazaki, and S. Oya, *Sen'i Gakkaishi*, **28**, 61 (1972).
- (4) T. Kitao, K. Yamada, T. Yamazaki, and S. Oya, *Sen'i Gakkaishi*, **28**, 221 (1972).
- (5) P. D. Griswold, A. E. Zachariades, and R. S. Porter, *Polym. Eng. Sci.*, **18**, 861 (1978).
- (6) A. E. Zachariades, W. T. Mead, and R. S. Porter, "Ultra-High Modulus Polymers", A. Ciferri and I. M. Ward, Eds., Applied Science Publishers, Essex, England, 1979, pp 77–116.
- (7) A. E. Zachariades, E. S. Sherman, and R. S. Porter, *J. Polym. Sci., Polym. Lett. Ed.*, **17**, 255 (1979).
- (8) M. C. Lang, C. Noel, and P. P. Legrand, *J. Polym. Sci., Polym. Phys. Ed.*, **15**, 1319 (1977).
- (9) L. Mandelkern, F. A. Quinn, and P. J. Flory, *J. Appl. Phys.*, **25**, 830 (1954).
- (10) C. H. Porter and R. H. Boyd, *Macromolecules*, **4**, 589 (1971).
- (11) D. B. Beech and C. Booth, *J. Polym. Sci., Part B*, **8**, 731 (1970).
- (12) E. Nedkov, M. Kreteva, M. Mihailov, and U. Todorova, *J. Macromol. Sci., Phys.*, **B21**, 371 (1982).
- (13) C. P. Buckley and A. J. Kovacs, *Prog. Colloid Polym. Sci.*, **58**, 44 (1975).
- (14) J. Clements, G. Capaccio, and I. M. Ward, *J. Polym. Sci., Polym. Phys. Ed.*, **7**, 693 (1979).
- (15) M. Jaffe and B. Wunderlich, "Thermal Physics", Vol. 17, R. F. Schwenker and P. D. Garm, Eds., Academic Press, New York, 1969.
- (16) P. Meares, "Polymers: Structure and Bulk Properties", Van Nostrand-Reinhold, London, 1965.
- (17) L. Mandelkern, *J. Appl. Phys.*, **26**, 443 (1955).
- (18) J. H. Southern and R. S. Porter, *J. Macromol. Sci. Phys.*, **B4**, 541 (1970).
- (19) W. T. Mead and R. S. Porter, *Int. J. Polym. Mater.*, **7**, 29 (1979).
- (20) S. M. Aharoni and J. P. Sibilia, *J. Appl. Polym. Sci.*, **23**, 133 (1979); *Polym. Eng. Sci.*, **19**, 450 (1979).
- (21) C. P. Buckley and A. J. Kovacs, *Colloid Polym. Sci.*, **254**, 695 (1976).
- (22) W. A. Miller, R. G. Shaw, and P. A. King, U.S. Patent 3941865.
- (23) S. Enomoto and M. Asahina, *J. Polym. Sci.*, **59**, 113 (1962).
- (24) I. Sakurada, T. Ito, and K. Nakamae, *J. Polym. Sci., Part C*, **15**, 75 (1966).
- (25) D. C. Bassett, "Principles of Polymer Morphology", Cambridge University Press, England, 1981.
- (26) W. G. Perkins and R. S. Porter, *Polym. Eng. Sci.*, **16**, 200 (1976).
- (27) P. J. Flory, *J. Am. Chem. Soc.*, **67**, 2048 (1945).
- (28) G. L. Wilkes, *J. Macromol. Sci., Chem.*, **C10**, 149 (1974).
- (29) I. M. Ward, "Mechanical Properties of Solid Polymers", Wiley, London, 1971.
- (30) G. Capaccio, T. A. Crompton, and I. M. Ward, *J. Polym. Sci., Polym. Phys. Ed.*, **18**, 301 (1980).